**Advances in Materials Research,** *Vol. 15, No. 2 (2026) 145-165*
https://doi.org/10.12989/amr.2026.15.2.145

Techno-Press

# Diagonal compression behaviour of cement-clay interlocking hollow brick masonry walls: Experimental and analytical assessment

Maddikera Lokanath Reddy*, Lingeshwaran N[a]

*Department of Civil Engineering, Koneru Lakshmaiah Education Foundation (Deemed to be University), Green Fields, Vaddeswaram, Guntur District, Andhra Pradesh, India - 522 302*

*(Received January 14, 2026, Revised April 20, 2026, Accepted April 21, 2026)*

**Abstract.** In this study, the diagonal compression behavior of cement-clay interlocking hollow brick (CCIHB) masonry walls is investigated using a combination of experimental and analytical study. The four wall configurations on full scales are considered: unreinforced - ungrouted, grouted, reinforced and grouted with vertical reinforcement. Diagonal compression tests were conducted as per ASTM E519 to measure in-plane shear strength, stiffness characteristics and failure modes. An analytical macro-modelling framework consisting of finite element plate representations for the masonry material, material zoning to simulate grout infill and embedded elements to simulate the vertical reinforcement. Analytical predictions are validated based on comparison of load vs displacement response, stress-based failure indicators, shear stress distribution, and global deformation patterns. The analytical results showed good agreement with experimental observations with peak load values predicted within 5% to 8% of measured values. Incorporation of grout infill increased the diagonal shear capacity by about 95% compared to ungrouted configuration and vertical reinforcement increased post-cracking resistance and deformation capacity. The combined grouted and reinforced wall system was shown to have the highest strength, stiffness, and ductility. Stress distribution patterns derived from the analytical models were found to be in qualitative agreement with those experimentally observed crack initiation and failure modes. The results validate the important role of the grout and reinforcement in enhancing the in-plane shear performance of CCIHB masonry walls and demonstrate the suitability of the proposed macro-modelling approach to capture their global structural behavior. This study forms a basis for the validated analysis in the assessment and design of interlocking masonry wall systems in sustainable and modular construction applications.

**Keywords:** cement-clay interlocking hollow bricks; diagonal compression; finite element analysis; STAAD. Pro modelling; macro-modelling

## 1. Introduction

The increased attention to sustainable, low-carbon, and resource-efficient construction efforts in the world has increased the search to find the alternative masonry system that can minimize material consumption and achieve performance that is adequate in terms of sustainable use. One of such systems is the cement Clay interlocking hollow brick (CCIHB) masonry, which has become a

*Corresponding author, Ph.D., E-mail: maddikeralokanathreddy@gmail.com
[a]Assistant Professor, E-mail: lingesh1609@gmail.com

**Copyright © 2026 Techno-Press**

ISSN: 2234-0912 (Print), 2234-179X (Online)

potential solution because of the low mortar requirement, easier assembly, speediness in construction, and favorable thermal insulation, which makes them very appealing to build cheap and sturdier facilities in the developing and fast-urbanizing countries [1-3]. Although there are these benefits, structural use of CCIHB masonry has not been well characterized as an alternative due to in-plane shear behavior of the material, especially regarding diagonal compression loading, which is critically important for seismic and wind resistance.

Alternative to the traditional bonded masonry, interlocking systems are based on geometric interlocks, discrete contact interfaces and hollow cores, which has complex shear-transfer mechanisms, unlike traditional masonry assemblies [4-6]. The nonlinear stress redistribution and localization effects, which cannot be well determined based on classical masonry theories, are brought in these characteristics. ASTM E519 [4], which is known as diagonal compression testing, is a common procedure that is used to assess in-plane shear strength, stiffness, and cracking behavior in masonry panels because of the tensile stresses introduced on the diagonal which dictate shear-controlled failure modes [7-9]. Past studies on hollow and partially grouted masonry have shown that confinement, stiffness, and shear capacity may be improved through the incorporation of otherwise disjointed load paths through grout filler [10-12]. Equally, vertical reinforcement has been demonstrated to enhance post-cracking behavior, ductility and energy dissipation through filling cracks and redistribution of tensile stresses [13, 14]. Nevertheless, the combined effect of grout and reinforcement in the unique geometry of CCIHB systems has not been rigorously studied so far and the internal stress-flow processes of the given performance gains are mostly not quantified. Recent research has examined the compressive behavior of masonry materials and the effects of supplementary cementitious components on cementitious matrix performance [15].

Finite element analysis (FEA) is a strong framework that can develop the knowledge on masonry behavior. Although the explicit nature of unit mortar interface behavior can be thought of using detailed micro-modelling techniques, these rely on several restricted computational resources, complicated constitutive modelling, as well as expert knowledge and understanding, making them unsuitable in standard engineering application [16-18]. Therefore, macro-modelling approaches which use homogenized continuity or plate elements have become more popular as viable alternative which can compute global structural response with much lower computational cost [19].

STAAD.Pro has found extensive use in the real world of structural engineering to analyse concrete and steel structures; however, there is little use of it on masonry, especially interlocking hollow brick masonry. Only isolated efforts of simplified masonry modelling have been reported to take place using STAAD.Pro and no reliable analytical framework has been developed to simulate the diagonal compression behavior of interlocking hollow brick panel and no comparison of analytical predictions against full-sized experimental outcomes had been made [20]. This corroboration limits the process of research and indeed the adoption of emerging interlocking masonry systems in practical designs.

The authors studied the four CCIHB wall configurations with the following loading stresses, taking the form of diagonal compression and these were unreinforced, unreinforced, reinforced and reinforced grouted as shown by the following abbreviations: W1, W2, W3 and W4. The observed outcomes of the experiment showed that the grout infill increased the in-plane shear strength twice, and the joint use of the grout and vertical reinforcement yielded the greatest stiffening, greater dissipation of energy, and broader distributions of crack ages. Although such results define physical performance properties of CCIHB masonry, the reliability of analytical tools in reproducing and predicting such behavior is yet to be validated.

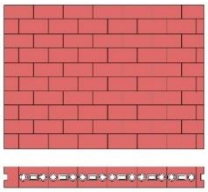

(a) W1 (URMW): Unreinforced masonry wall with ungrouted hollow cores

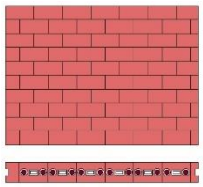

(b) W2 (URMW-G): Unreinforced masonry wall with vertical cores grouted

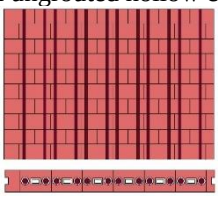

(c) W3 (RMW): Reinforced masonry wall with ungrouted hollow cores, containing vertical 8 mm Fe 500 rebars

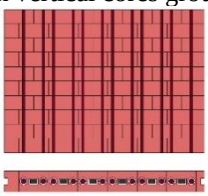

(d) W4 (RMW-G): Reinforced masonry wall with grouted vertical cores containing vertical 8 mm Fe 500 rebars

Figure 1. Specimen and Geometry configuration (W1–W4)

### 1.1 Research Gap

The critical analysis of the available literature introduces the following research gap of the CCIHB masonry walls will be subjected to a diagonal compression loading and the available analytical experimental correlation studies are non-existent. The infill and vertical reinforcement in a CCIHB system have not been analytically determined in terms of enhancement of stress flow inside the structures, enhancement of the stiffness, and progression of the failure. The STAAD. Pro has been seldom used in the analysis of shear in masonry and has not been verified in the analysis of interlocking hollow brick. An effective and repeatable macro-modelling methodology to be used in engineering practice during the performance-based evaluation of CCIHB walls does not yet exist. Unlike previous studies, the present work establishes a validated analytical experimental correlation framework for cement-clay interlocking hollow brick (CCIHB) masonry using an engineer-oriented STAAD. Pro based macro-modelling approach.

### 1.2 Novelty of the Study

To make this study, the following original contributions can be made:

• Formulation of first validated STAAD. Pro-based macro-modelling framework to predict the behavior of CCIHB masonry wall compressive behavior, in the diagonal.

• An analytical-experimental comparison of all these: load-displacement response, stiffness properties, shear stress distribution, principal tensile stress contours, and the predicted cracking behavior.

• Refined conceptualizations of the purpose of grout infill and vertical supporting in alteration of the loads of internal stress pathways, confinement effects as well as localization of failure in interlocking masonry systems.

This will provide a viable, engineer-friendly modelling process that can be easily incorporated to analyse and optimise the design of interlocking masonry walls.

### 1.3 Objectives

The objectives of this study are specific in that they are to:

• Formulate STAAD. Pro macro-models using finite element analysis of the four experimentally tested CCIHB wall configurations.

• Diagonal compression loading Simulate based on ASTM E519 and obtain the most important structural response parameters.

• Compare the results of analytical prediction and experimental results in terms of peak strength, stiffness, and cracking behavior.

• Measure the individual and combined action of grout infill and vertical reinforcement on the performance of CCIHB masonry walls about in-plane shear.

• Forward a confirmed and sizeable generalizable modelling system to propose future data and superstructure plan of interlocking masonry frameworks.

This research thus fills the much-required gap by correlating serious experimental data with a proven analytical measurement methodology and offers a sound and scaly foundation of knowledge in comprehending and developing the next-generation sustainable interlocking masonry system.

## 2. Methods

Developed a full-scale experimental programme to explore the behavior of cement clay interlocked hollow and brick walls in a diagonal compression. The findings of this research are the yardstick to confirm the analytical modelling undertaken in this paper. The main points of the experimental methodology are not described here, only essential points. Material-level effects of metal waste incorporation on cementitious bond behavior have been demonstrated in timber/metal hybrid concrete systems [21].

### 2.1 Materials

#### 2.1.1 Cement Clay Corrugated hollow brick

Wall specimens manufactured in the CCIHB units were of size is 250 × 125 × 100 mm and two hollow cylindrical cores (60 mm diameter) were used vertically. The mean compressive strength of single bricks was 6.7 MPa having water absorption of 14.5%. These characteristics guaranteed the stability of masonry activity at all trial specimens.

#### 2.1.2 Mortar

The bed and head joints were laid using 1:4 cement and sand mortar. The compressive strength of the mortar cubes was 22.1 MPa after 28 days which is satisfactory making sure that the quality of bonds and workable consistency in the construction of the wall.

#### 2.1.3 Grout

In the case of grouted specimens, a base of slump 220 mm of cement/sand mix was utilized to achieve full cage fill up of the hollow cores. The compressive strength of the grout was 28.5MPa, 28 days later.

#### 2.1.4 Reinforcement

Vertical reinforcement, which was 8 mm diameter Fe 500 steel rebars, were located at the

Table 1. Specimen Configurations

| Specimen ID | Grout | Vertical Reinforcement | Description |
|---|---|---|---|
| W1 | No | No | Unreinforced, Ungrouted (control) |
| W2 | Yes | No | Grouted cores only |
| W3 | No | Yes | Reinforced cores without grout |
| W4 | Yes | Yes | Grouted and reinforced (composite system) |

center of the hollow cores in the corresponding specimens. The results of the measured yield strength were 520 MPa, and the elastic modulus was 200 GPA.

All masonry units were constructed under controlled laboratory conditions to ensure consistency across specimens. The mortar and grout mixes were prepared using a mechanical mixer to achieve uniform consistency. Dry constituents were first mixed thoroughly, followed by the gradual addition of water to obtain the desired workability. After casting, all wall specimens were kept under ambient laboratory conditions for 24 hours to allow initial setting. Subsequently, the specimens were cured for 28 days under controlled conditions to ensure proper hydration and strength development. During this period, adequate moisture was maintained to minimize shrinkage effects. The construction of wall panels was carried out with careful control of alignment and joint thickness. The bed and head joints were maintained at a nominal thickness of 10 mm with a tolerance of ±2 mm to ensure uniform stress distribution. Vertical alignment and dimensional accuracy of the panels were verified during construction to minimize geometric imperfections. These procedures were adopted to ensure repeatability and reliability of the experimental results.

## 2.2 Specimen Configurations

The four-square panels of the wall were built on a running bond structure in 10 mm mortar joints and measuring 1000 × 1000 × 125 mm. The settings were as Table 1.

## 2.3 Test Setup and Instrumentation

All the panels were subjected to diagonal compression as per ASTM E519/E519M-15.

A compressive loading of each specimen along the vertical diagonal of the diagonal displacing it by 45° was performed using steel bearing shoes to provide the panel with a uniform shear field.

Instrumentation

• Two LVDTs were placed on compression and tension diagonals to check the shortening and lengthening.

• Load application to avoid loading the spring under displacement control, a hydraulic jack has been used at 0.5 mm/min.

• A load cell that was calibrated was used to measure the loads at the condition of 10 Hz frequency.

• C- Initiation, propagation, and patterns of failure of the crack were visually recorded.

• Such arrangement made it possible to correctly measure shear stress, shear strain, initial stiffness, and post-peak behavior.

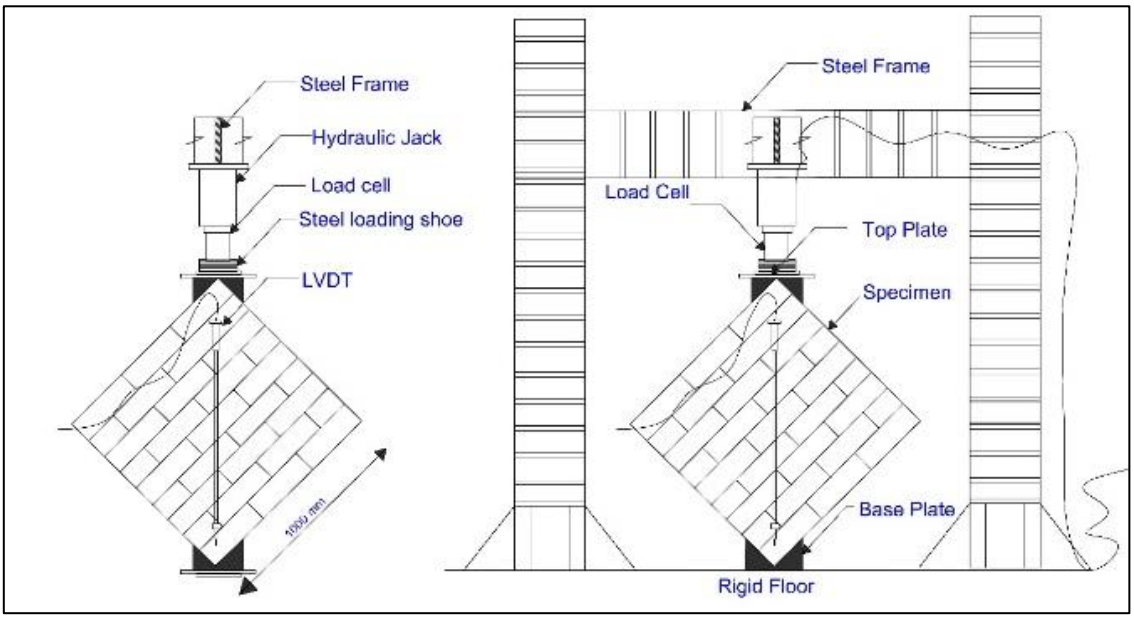


Figure 2. Construction / Assembled Wall Panels

Table 2. Summary of Experimental Results

| Specimen ID | Peak Load (kN) | Initial Stiffness (kN/mm) | Peak Shear Stress (MPa) |
|---|---|---|---|
| W1 | 38.5 | 3.1 | 0.31 |
| W2 | 75.2 | 6.4 | 0.61 |
| W3 | 52.1 | 4.2 | 0.42 |
| W4 | 83.6 | 7.1 | 0.68 |

### 2.4 Test Setup and Instrumentation

The main results obtained from the experimental program are summarized in Table 2.

Failure Characteristics

- The failure mode of W1 is brittle with a single diagonal crack.
- There were several cracks that were distribution cracks in W2 because of grout confinements.
- W3 displayed a crack-bridging reinforcement behaviour, although not confined.
- W4 formed good distribution of cracking and demonstrated the greatest ductility and strength.

These experimental results give the required standard, by which predictive power of the STAAD. Pro analysis models described in the following section can be assessed.

## 3. Analytical Modelling in STAAD. Pro

STAAD. Pro CONNECT Edition developed a finite element (FE) macro-modelling framework that was used to simulate the diagonal compression behaviour of CCIHB wall panels. This analytical model is a copy of the geometry, boundary conditions, material composition, and loading arrangement of the experimental studies which allows meaningful analytical experimental

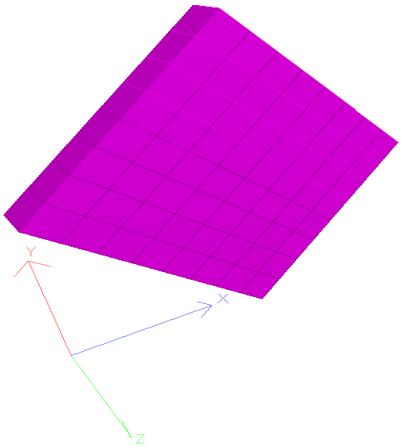

Figure 3. FE Model Geometry

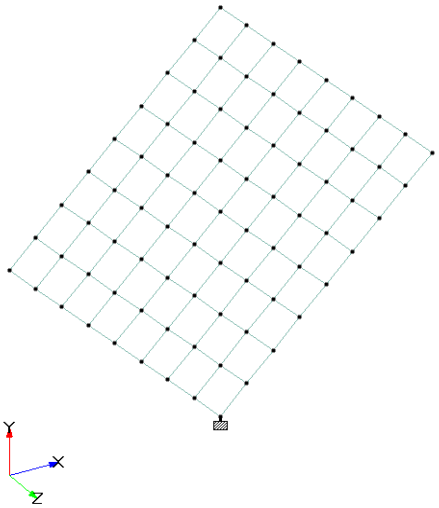

Figure 4. Mesh Layout

validation. The modelling methodology is based on the principles of the macro-modelling of masonry in that the plate elements are homogeneous, the material is assigned to the region, and the reinforcement is modelled by part of the timber [1, 2].

### 3.1 Modelling philosophy and assumptions

A macro-modelling approach is used, by which the masonry panels are treated as a homogenous continuum and are represented using plates. This approach is applicable to global response prediction of load vs displacement history, shear stress distribution and crack initiation while being much more computationally efficient than micro-modelling.

The following assumptions were used:

• An equivalent linear-elastic orthotropic material is used for masonry.

Table 3. Material Properties Used in the Analytical Model

| Material | Elastic Modulus (E) | Poisson's Ratio (ν) | Density (kg/m³) |
|---|---|---|---|
| Masonry | 1500 MPa | 0.20 | 1800 |
| Grout | 7000 MPa | 0.22 | 2100 |
| Steel reinforcement | 200,000 MPa | 0.30 | 7850 |
| Material | Elastic Modulus (E) | Poisson's Ratio (ν) | Density (kg/m³) |

• Difference in grouted cores is treated as higher one then of the plates mesh.
• The reinforcement is modelled as an embedded beam element with full bond.
• Damage and cracking are assumed from principal tensile stress contours, rather being modelled explicitly through material degradation.
• Dominant is the in-plane behaviour Out of plane effects will here be neglected.

### 3.2 Model geometry and element discretization

The wall panel was simulated as a 1000 × 1000 × 125 mm square plate which is the same size with the tested specimens. The panel was placed at 45° when rotated around the STAAD axis so that the diagonal compression condition could be exactly simulated.

Element Selection

• PLATE MAT elements were adopted to simulate the masonry continuum.
• The Finite Element Mesh - A structured mesh was used with element sizes of 25 to 40 mm to achieve a good compromise between accuracy and computational expense.
• Local meshing refinement was carried out in the regions of grout and reinforcement to obtain a better strain resolution.

### 3.3 Material property assignment

Equivalent material properties for masonry were derived from experimental stiffness values, ensuring the model reproduces realistic initial deformation.

The equivalent modulus for masonry was calibrated using the initial stiffness of W1 from the experimental results, ensuring consistency in the elastic response.

The equivalent elastic modulus of masonry ($E_{eq}$) adopted in the analytical model was calibrated using the experimentally obtained initial stiffness of the control specimen (W1). The initial stiffness, $K$, was evaluated from the linear elastic region of the load–displacement response obtained from the diagonal compression test.

The relationship between stiffness and material properties was expressed as:

$$K = \frac{P}{\Delta}$$
$$E_{eq} = \frac{K \cdot L}{A} \quad (2)$$

where P is the applied load, Δ is the corresponding displacement, Lis the effective diagonal length of the panel, and Ais the effective cross-sectional area.

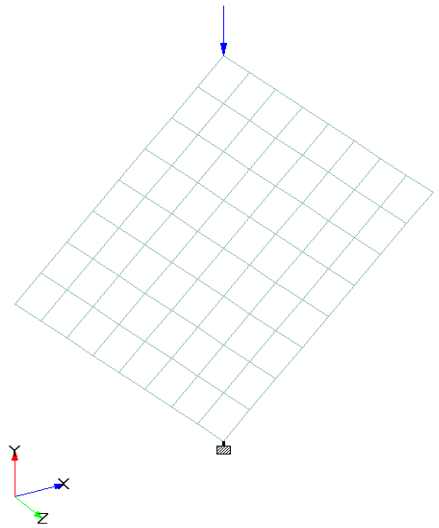


Figure 5. Boundary Conditions and Loading

This calibration procedure ensures consistency between the experimentally observed elastic response and the analytical model. The control specimen (W1) was selected for calibration as it represents the intrinsic behaviour of the masonry system without the influence of grout or reinforcement. Based on this approach, the equivalent modulus used in the analysis was determined as 1500 MPa.

### 3.4 Boundary conditions and support representation

The setup described in the ASTM E519 procedure was mimicked by the incorporation of boundary conditions. Bottom Bearing Shoe

- Fixed in all translation (UX, UY, UZ).
- No restrictions are placed on rotations (RX, RY, RZ) to prevent an artificial moment constraint.
- Top Bearing Shoe Rigidly attached to the panel nodes to provide uniform application of the load.
- Applied in the global vertical direction to act as a diagonal compression.
- Movements in the horizontal direction and the out-of-plane direction were fixed.

These support conditions allow to attain a shear-dominant response that aligns with the response from the experimental studies.

### 3.5 Loading application and output parameters

Displacement controlled incremental analysis was used to apply diagonal compression loading to capture the degradation of stiffness and the post-peak response in a stable manner. Corresponding to the experimental configuration of loading, the load was applied to the top corner node that lies along the diagonal of the panel. The increment of the load step was chosen based on the need for

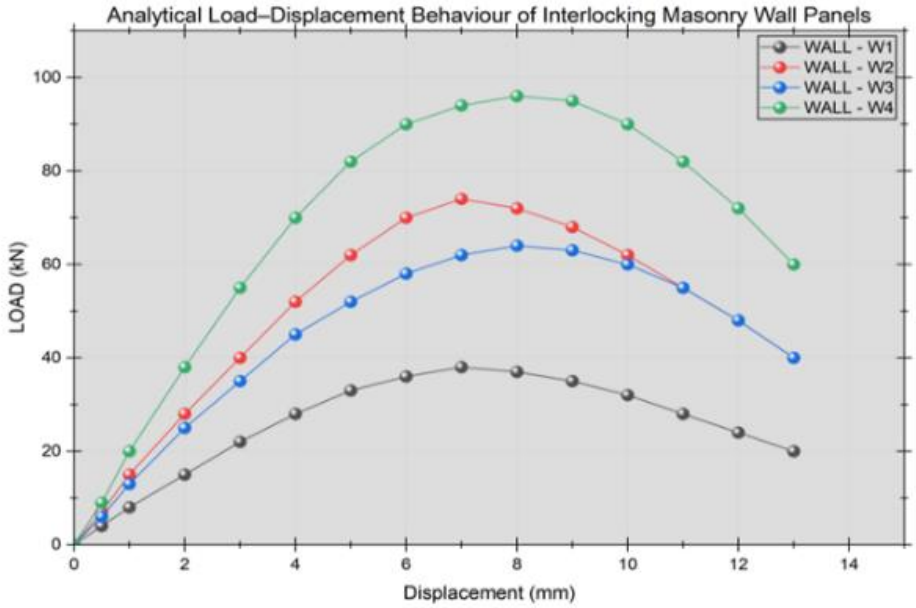


Figure 6. Analytical load vs displacement response of CCIHB wall panels (W1–W4) under diagonal compression

convergence of the numerical solution, as well as the need to adequately resolve the load–displacement response. The diagonal displacements were tracked to produce analytical load–displacement relationships, while the reaction forces were stored for each increment. Once a reduction of tangent stiffness was sufficient, the loading was stopped due to the structural failure of the specimen. Incremental analysis response parameters were extracted directly from the software, as well as the overall response parameters including the load–displacement response, the overall response stiffness, and the maximum response load to determine the peak load achievement.

In addition to the overall response parameters, the internal response mechanisms were evaluated and more specifically the internal failure mechanisms using stress response indicators. These stress indicators included principal tensile stress ($\sigma_1$) contour maps to determine the zones in which cracks would form and in-plane shear stress ($\tau xy$) maps to clarify the mechanisms by which shear was transported. The outputs were used to compare with experimental results and the results specifically to explain the behaviour during diagonal compression.

## 4. Results

The analytical results to be discussed here stem from the STAAD.Pro macro-models of the CCIHB wall panels under diagonal compression. We analyse the results by focusing on the global response characteristics of the wall panels, the accuracy of strength prediction, the internal mechanisms of stress transfer and the deformation characteristics. To assess the validity of the proposed modelling framework, the analytical results must be compared with the experimental results.

Table 4. Analytical Simulations

| Specimen | Experimental (kN) | Analytical (kN) | Difference (%) |
|---|---|---|---|
| W1 | 38.5 | 36–40 | < 5% |
| W2 | 75.2 | 70–80 | < 7% |
| W3 | 52.1 | 50–56 | < 8% |
| W4 | 83.6 | 80–90 | < 6% |

### 4.1 Load vs displacement behaviour

Panel displacement was measured on the load application column, and the panel's force reaction was measured at the loading point. All those specimens behaviour exhibited an overall initial linear response and then followed stages where they showed diagonal cracking first. All those specimens exhibited some initial linear response and followed those responses with stiffness degradation with diagonal tension cracking. The two (2) blocks which did not contain reinforcement, and which did not contain grout, had the lowest initial peak response and stiffness. But the overall response was a post shear and a rapid decrease in response, indicating a response of brittle shear dominated failure which was dictated by tension and diagonal cracking along a singular load column. Grouting increased the remaining stiffness and peak response to a significant degree. Grouting showed the analytical response to have a better post-peak behaviour, indicating an overall better performed responsive system. The panel which was reinforced and did not contain grout was better in overall response by a moderate degree with respect to the Block of Wall response and had a better post cracking response indicating an overall cohesive reinforcement of the system. The configuration in which the panel contained bonded reinforcement and used grout, which showed the highest deformation capacity, peak load response, and load column displacement, also had the most responsive system where the post behaviour showed little change with a plateau which indicated the response was dominated by the system overall cohesive behaviour.

### 4.2 Peak load comparison

As shown in Table 4, the peak loads from the analytical simulations were compared with the experimental values. The analytical framework also successfully matched the experimental strength hierarchy (W4 > W2 > W3 > W1), which further emphasizes the predictive success of the analytical framework in identifying the dominant shear-resisting mechanisms. The small differences can be explained by the assumptions of homogenised material and the lack of explicit nonlinear cracking, which are all standard limitations of continuum-based macro models.

### 4.3 Principal Tensile Stress ($\sigma_1$) Contours

In W1, $\sigma_1$ stresses were concentrated on a narrow diagonal band, ranging from the loaded to supported corners, aligned with the appearance of the single predominant diagonal crack. This pattern supports the brittle character of shear failure in unreinforced, ungrouted interlocking masonry. In W2, ungrouted masonry, the infill of the grout reduced the peak concentrations of $\sigma_1$, as well as the relocation of the stress concentrations, resulting in a wider band of stress distribution and a longer time to the initiation of a crack. This explains the observed increase in stiffness and

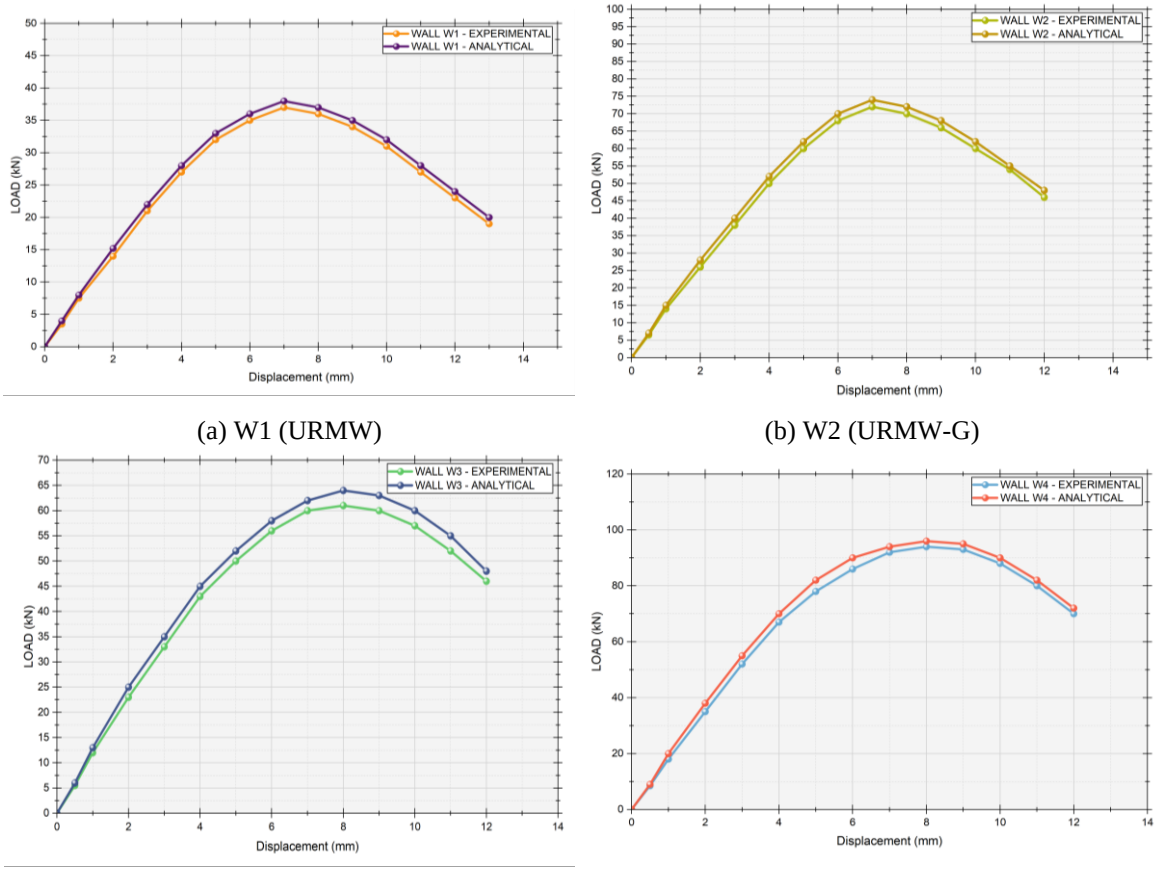


(a) W1 (URMW) (b) W2 (URMW-G)

(c) W3 (RMW) (d) W4 (RMW-G)

Figure 7. Comparison of experimental and analytical load–displacement responses for CCIHB wall panels under diagonal compression

strength in comparison to W1. In W3, the addition of reinforcement yielded some level of stress transfer across the cracked sections and thereby reduced the localised concentration of $\sigma_1$ cracks and enabled a more incremental controlled pattern of cracks. The reasonably unreinforced portions of masonry were able to bridge the diagonal cracks and redistribute the tensile stresses after the cracking process. W4 exhibited the most distributed $\sigma_1$ field, with the presence of several pathways for stress with little to no concentration of stress. This is indicative of a robust integrated load transfer system, aligned with the experimental manifestation of distributed cracking and a ductile nature of the failure.

The peak principal tensile stress observed in the unreinforced specimen (W1) was highly localized along a narrow diagonal band. In contrast, grouted and reinforced configurations (W2–W4) exhibited a noticeable reduction in stress concentration, with peak $\sigma_1$ values reduced by approximately 20–40% and distributed over a wider side of the panel. This reduction indicates improved stress redistribution and delayed crack localization due to the presence of grout and reinforcement.

Principal tensile stress contours are presented in Fig. 8 for all specimens.

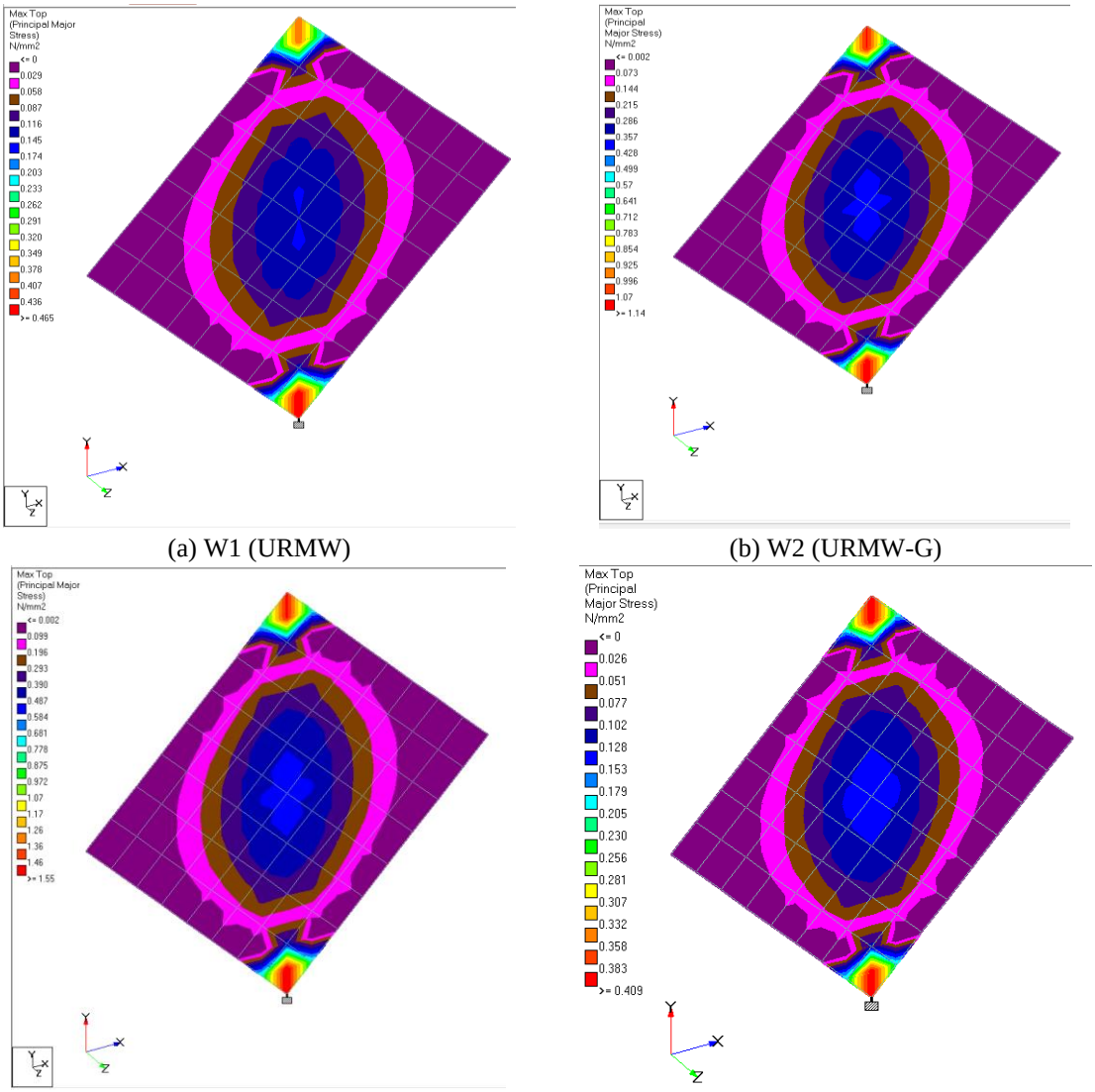


(a) W1 (URMW) (b) W2 (URMW-G)

(c) W3 (RMW) (d) W4 (RMW-G)

Figure 8. Principal Tensile Stress ($\sigma_1$) Contours

Fig. 10 shows shear stress ($\tau xy$) contours produced from different analytical shear-transfer models. Shear behaviour mechanisms governing the response of the CCIHB panels. With an ungrouted and unreinforced configuration (W1), shear stresses highly localize along a narrow diagonal load path and leads to premature localization and brittle shear failure. With the inclusion of grout in W2, the shear concentrating zone significantly increased because of an effective shear resistance zone gradation attained because of greater stiffness continuity across the hollow cores, which decreased peak shear concentration and a more uniform shear stress distribution. In W3, vertical reinforcement also contributed to the shear resistance indirectly by shear-transferring/ redistributing tensile forces along brittle, cracked regions and thus, reduced the local shear demand

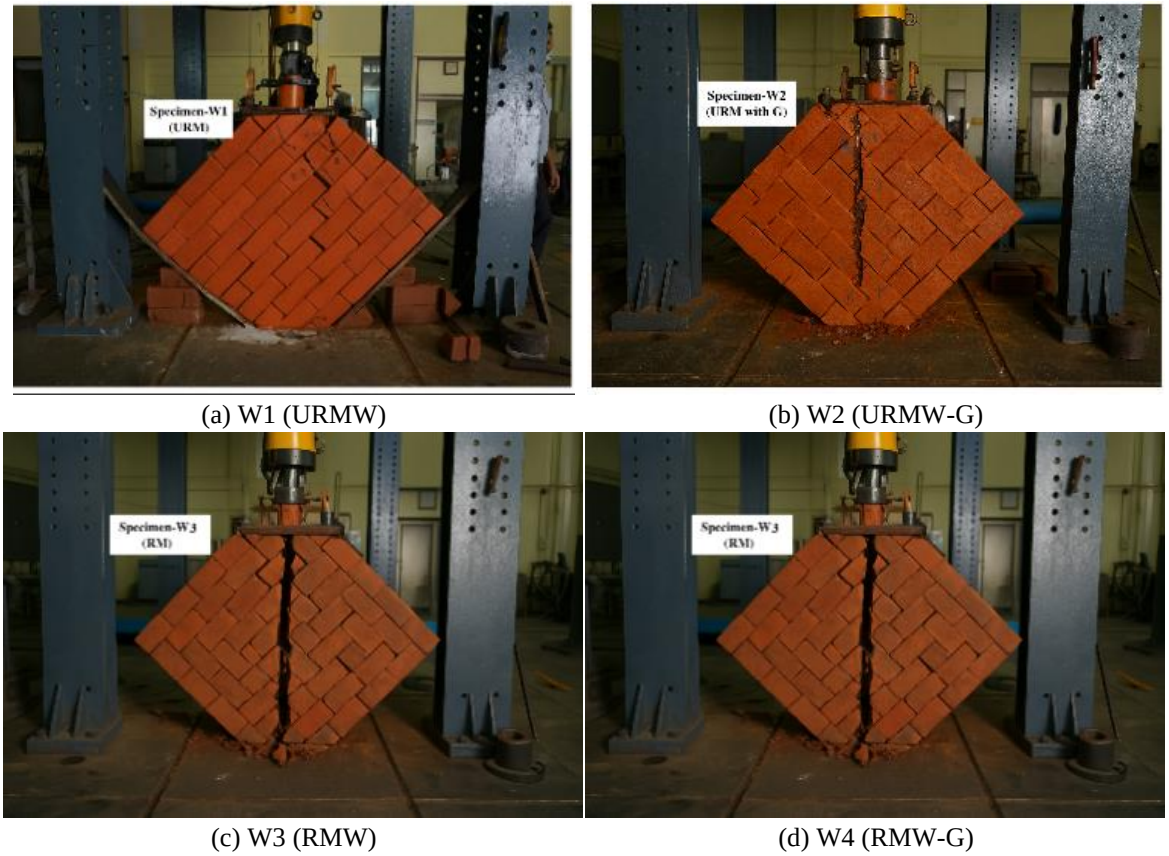


(a) W1 (URMW) (b) W2 (URMW-G)

(c) W3 (RMW) (d) W4 (RMW-G)

Figure 9. Representative cracking patterns and failure modes of W1–W4 specimens

closer to the diagonal crack. The configuration of grout and reinforcement (W4) had the most uniform τxy distribution, confirming the load transfer across the panel and shear stress distribution because of the synergistic interaction of grout confinement and reinforcement. The increased transfer of shear stress explains the increased shear capacity and increased deformation stability from W1 to W4.

A similar trend was observed in the shear stress distribution. The ungrouted configuration (W1) exhibited high shear stress concentration along a narrow load path, whereas the inclusion of grout and reinforcement led to a more uniform distribution. The effective shear transfer zone increased significantly in W2–W4, with a corresponding reduction in peak τxy values and lower stress gradients across the panel. This behaviour reflects enhanced load-sharing mechanisms and improved structural integrity in the composite systems.

### 4.4 Shear Stress (τxy) Distribution

Fig. 10 shows shear stress (τxy) contours produced from different analytical shear-transfer models. Shear behaviour mechanisms governing the response of the CCIHB panels. With an ungrouted and unreinforced configuration (W1), shear stresses highly localize along a narrow diagonal load path and leads to premature localization and brittle shear failure. With the inclusion

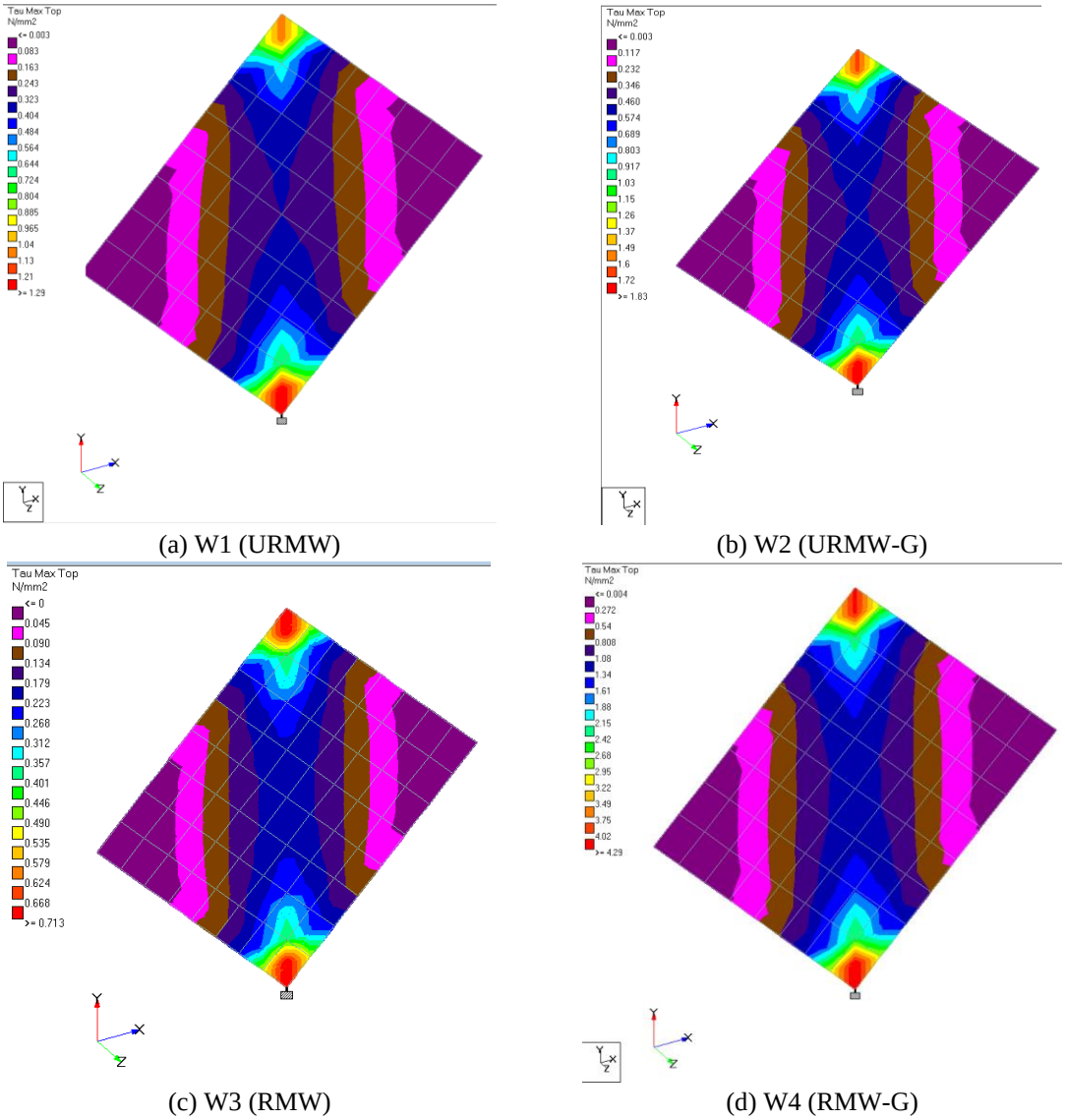


(a) W1 (URMW) (b) W2 (URMW-G)

(c) W3 (RMW) (d) W4 (RMW-G)

Figure 10. Shear Stress (τxy) Contours

of grout in W2, the shear concentrating zone significantly increased because of an effective shear resistance zone gradation attained because of greater stiffness continuity across the hollow cores, which decreased peak shear concentration and a more uniform shear stress distribution. In W3, vertical reinforcement also contributed to the shear resistance indirectly by shear-transferring/ redistributing tensile forces along brittle, cracked regions and thus, reduced the local shear demand closer to the diagonal crack. The configuration of grout and reinforcement (W4) had the most uniform τxy distribution, confirming the load transfer across the panel and shear stress distribution because of the synergistic interaction of grout confinement and reinforcement. The increased transfer of shear stress explains the increased shear capacity and increased deformation stability

from W1 to W4.

A similar trend was observed in the shear stress distribution. The ungrouted configuration (W1) exhibited high shear stress concentration along a narrow load path, whereas the inclusion of grout and reinforcement led to a more uniform distribution. The effective shear transfer zone increased significantly in W2–W4, with a corresponding reduction in peak τxy values and lower stress gradients across the panel. This behaviour reflects enhanced load-sharing mechanisms and improved structural integrity in the composite systems.

The experimental crack patterns for comparison are shown in Fig. 9.

### 4.5 Summary of analytical performance

The analytical models replicated the essential traits of the experiments, including the peak load capacity, initial stiffness, load versus displacement behaviours, and the stress and deformation characteristics of the material. The close correspondence of the analytical and experimental data underscores the capability of the STAAD.Pro, macro modelling framework, to characterize the phenomena controlling the diagonal compression response of CCIHB block walls.

## 5. Discussion

Analytical and experimental findings are discussed to explain the main mechanisms influencing the CCIHB masonry walls diagonal compression behaviour. The grout infill and vertical reinforcement acting separately and together, the proposed macro-modelling framework, and the structural engineering and practical applications are all addressed.

The experimental programme was designed using a controlled parametric approach with four wall configurations to isolate the individual and combined effects of grout infill and vertical reinforcement. Each specimen represents a distinct structural condition, enabling direct comparison of governing behavioural mechanisms.

While the number of specimens is limited, the selected configurations are sufficient to capture the primary variables influencing the diagonal compression response of CCIHB masonry. The focus of the study is on mechanistic interpretation and validation of the analytical modelling framework rather than statistical generalization of material variability.

Such an approach is commonly adopted in masonry research, where well-defined representative specimens are used to investigate fundamental behaviour under controlled conditions. The findings of this study therefore provide a reliable basis for understanding system behaviour and for developing validated analytical models.

### 5.1 Influence of grout on structural behaviour

The grout infill contributes significantly to the increased stiffness and diagonal shear capacity of the CCIHB masonry walls. Among the specimens, those with grout (i.e. W2 and W4) were statistically significantly stiffer and stronger than those without grout. The reason for this is likely the inclusion of hollow grout cores, which enable individual masonry walls to act as a cohesive and continuous system. The grout infill allows for a redistribution of diagonal shear and internal tensile stresses, thereby reducing any localized stress. This response explains the behavioural change i.e. brittle failure, observed during the experiments, where a single dominant diagonal

shear crack transitioned to multiple diagonal shear cracks. Confinement-induced improvements and similar behavioural response to the ones in the present study has also been previously reported in the case of hollow masonry units with grout and partially filled masonry walls [10–12]. This study also demonstrates that grout infill within CCIHB walls improves damage tolerance, ductility in shear dominant loads, and overall engineering behaviour.

### 5.2 Influence of vertical reinforcement

When implemented severally, vertical reinforcement affected post-cracking behaviour more than peak shear strength. As compared to the unreinforced control specimen (W1), the reinforced but ungrouted specimen (W3) showed improved load retention, smoother stiffness degradation, and delayed crack initiation.

These benefits are because of reinforcement crack-bridging, which redistributes tensile stresses and restrains opened cracks across cracked regions. The effects of this were captured analytically through decreased $\sigma_1$ localization and moderated $\tau xy$ concentrations along the failure zone diagonal. That W3 also performed lower than the grouted specimen (W2) suggests that in the absence of confinement, reinforcement alone cannot meaningfully improve diagonal shear resistance. This is in line with prior evidence pursued in reinforced masonry, which notes that as the confinement and bond conditions dampen, the effectiveness of the reinforcement also diminishes [13, 14]. The results obtained have revealed that more than providing a substitute for the stiffness enhancement brought about by grouting, reinforcement is more effective in terms of post peak stability and ductility.

### 5.3 Composite action in grouted and reinforced systems

Composite actions with grouting and reinforcing elements (W4) develop best overall performances in all parameters suggesting optimal unit composite interaction of masonry, grout and vertical reinforcements. Stress field analyses show overall redistributed tension and shear stresses with a broader deformation controlled without significant localised stress concentrations.

This was experimentally seen with overall ductility and a stable carry-over of the load with the formation of a greater overall length of cracks. These composite actions resulting in ductility confirm the continuity of confinement, and the presence of reinforced load-bridging mechanisms with tension. Stiffness and confinement were contributed by the grout, and the reinforcements governed overall post-crack stability, with controlled shear without loss of performance. This composite synergistic mechanism, related to the in-plane shearing of composite solid masonry, suggests a greater unit-joint performance and has been well documented in literature [11, 14]. This composite synergistic behaviour shows the potential of macro-modelling to depict interlocking masonry systems with multiple components. The enhanced strength response in composite masonry materials is consistent with previous observations for modified cementitious systems and masonry unit compressive behavior in published studies [22].

### 5.4 Analytical–experimental correlation and model fidelity

All wall configurations revealed that the analytical predictions matched the actual behaviour of specimens for the load–displacement response, peak shear capacity, characteristics of the deformation, and modes of failure.

The analytical and experimental peak loads differed by a margin of 5–8% which is a typically accepted error margin for homogenised macro-modelling approaches that do not explicitly capture discrete cracking and bond–slip behaviour [16-18]. Crucially, the contradiction of the predicted analytical localization zones of $\sigma_1$ and the observed experimental crack paths supports the idea of using stress indicators for inferring failure mechanisms in interlocking masonry. Although the model does not explicitly account for crack propagation, the model's ability to predict the primary stress trajectories and the overall response patterns is sufficient to conclude that the model is valid for the purpose of performance benchmarking. The same validation approaches described here have been reported in macro modelling of masonry walls which have been subjected to in-plane loading [17-19].

In addition to the direct comparison with the present experimental results, the analytical predictions were evaluated against behavioural trends reported in existing studies on interlocking and grouted masonry systems. Previous investigations have consistently shown that grout infill significantly enhances shear strength and stiffness by improving internal load transfer and confinement, while vertical reinforcement primarily contributes to post-cracking resistance and ductility.

The analytical results obtained in this study exhibit the same response hierarchy and performance trends, with grouted and reinforced configurations demonstrating superior strength, stiffness, and deformation capacity. This agreement with established findings in the literature provides additional confidence in the predictive capability of the proposed STAAD.Pro-based macro-modelling framework [23-25].

Although direct benchmark studies on CCIHB systems are limited, the consistency of the analytical results with widely reported masonry behaviour indicates that the modelling approach is robust and can be reliably extended for practical engineering applications.

### 5.5 Mechanistic interpretation of diagonal compression behaviour

The experimental and analytical research has provided a clear understanding of the mechanics of diagonal compression behaviour in CCIHB Masonry Walls. Unreinforced and ungrouted masonry happens due to a localised diagonal tensile cracking failure; this happens because there is limited tensile failure and a lack of confinement. Grout fills help in the resistance of the load core system as it redistributes the stresses, increases stiffness and strength, and fills the hollow zones of the system. While vertical reinforcement contributes to resistance to post-cracking, it contributes resistance to deformation stability as it is most efficient in combination with confinement that is due to grout. Fully composite systems show these simplified behaviours that result in the system having a greater overall strength, having greater overall stiffness, and having greater overall ductility. These behaviours show that the grout, reinforcement, and masonry units interactions affect the systems shear dominated response that is especially true for interlocking systems due to the difference of load transfer mechanisms compared to typical bonded masonry.

### 5.6 Implications for structural modelling and design

A similar STAAD. Macro-modeling frame adopted in the Pro and its prospect in engineering assessment of interlocking masonry system for practical application. The results suggest that plate-based homogenised modelling with region-specific material assignment and embedded reinforcement representation is sufficient to predict global response of members in diagonal

compression.

In terms of design, the results indicate that grouted and reinforced CCIHB walls may be an option as low-rise SRW in wind- and mild seismic-design regions if proper detailing and calibration are used.

### 5.7 Comparison with masonry design provisions

To assess the practical relevance of the experimental results, the obtained shear stress values were compared with typical design provisions for masonry systems. As per standard guidelines such as IS 1905 and Eurocode 6, the characteristic shear strength of conventional unreinforced masonry is generally limited to relatively low values, depending on mortar strength and normal stress conditions.

In the present study, the peak shear stress of the control specimen (W1) falls within the expected range for unreinforced masonry. However, the grouted and reinforced configurations (W2–W4) exhibited significantly higher shear stress values, reaching up to 0.68 MPa. This enhancement indicates the beneficial effect of grout infill and reinforcement in improving shear resistance beyond conventional masonry limits.

Although direct code provisions for interlocking hollow brick masonry are not explicitly available, the observed improvements suggest that such systems, when properly detailed, can achieve superior structural performance compared to traditional masonry. These findings support the potential inclusion of CCIHB systems in performance-based design approaches.

### 5.8 Limitations and future research

While the present study demonstrates promising results, certain limitations must be acknowledged. The analytical model assumes perfect bond between masonry units, grout infill, and reinforcement, whereas actual behaviour is governed by complex bond–slip mechanisms, particularly under post-cracking conditions. This simplification may result in slightly higher stiffness predictions and more uniform stress distributions compared to real systems. Additionally, material nonlinearity and damage evolution were represented using stress-based indicators rather than explicit constitutive models. The analysis was further limited to monotonic in-plane loading, with out-of-plane effects, cyclic loading, and dynamic behaviour not considered.

Despite these assumptions, the analytical predictions show good agreement with experimental results in terms of global response and failure patterns, indicating that the model is adequate for capturing overall structural behaviour. However, incorporation of more advanced modelling strategies would enhance predictive accuracy.

Future research should focus on integrating bond–slip behaviour through advanced interface modelling techniques to better represent stress transfer and crack propagation. The adoption of nonlinear material models, including elastoplastic behaviour in tension and anisotropic damage in compression, would further improve simulation fidelity. In addition, systematic parametric studies are recommended to evaluate the influence of grout strength, reinforcement ratio, and geometric parameters such as panel aspect ratio and thickness. Extension to cyclic and seismic loading conditions is also essential to assess structural performance under realistic service environments. These developments would contribute to more reliable analytical tools and support the design and practical implementation of interlocking masonry systems.

## 6. Conclusions

This work combined field-testing and analytical studies on the diagonal compression behaviour of CCIHB masonry walls. Using the STAAD.Pro modelling effort completed to a macro level and calibrated against full-scale tests and E519, the following conclusions can be advanced

• The presence of grout as a constituent of the infill was identified as the most significant cause of the elevation of the in-plane shear behaviour. Grout and wall configurations were found to possess, in addition to the improved confinement, integration of the hollow cores, and load-resisting system, significant increases in initial stiffness and peak shear capacity.

• The post-cracking behaviour and deformation capacity were improved by vertical reinforcement. This was attributed to the bridging of cracks and significant redistribution of stress. Reinforcement in walls, of itself, was found to be ineffective in the increase of peak shear strength unless grout confinement was present.

• The presence of vertical reinforcement and grout in a wall system composite action, and offered a superior wall system strength, stiffness, and ductility. The composite walls were predicted from the analytical models to be distributed cracking and stable post-peak phase, and the experimental composite walls conceded to analytical models, demonstrated consistent post-peak behaviours.

• Predictive capabilities of proposed STAAD.Pro-based macro-modelling frameworks were within 5-8% of the actual measure values. Stress indicators such as principal tensile were significant to provide insights into the internal load transfer mechanisms and the formation of cracks.

• The proposed methodology to assess the diagonal compression behaviour of interlocking masonry walls can be reproduced and applies analytical methods that make use of available software for structural analysis. It provides an alternative that is computationally efficient and that also fits the purpose of moderate precision for an overall response within the framework.

The interactions of the materials that impact the shear behaviour of interlocking masonry provide support for use of CCIHB walls that are grouted and reinforced on low-rise structures with the presence of in-plane loads.

The present study focused on monotonic diagonal compression. Future research should expand on incorporating bond–slip behaviour and nonlinear material damage, cyclic and seismic loading, and variations on the grout and reinforcement detailing. These would enhance analytical tools for the performance assessment and design of interlocking masonry.

## Acknowledgment

The authors express their sincere gratitude to the management and faculty of their institution for providing the necessary facilities and support to carry out this research work.

## References

1. Joyklad, P., Hussain, Q. (2019). Axial compressive response of grouted cement–clay interlocking hollow brick walls. Asian Journal of Civil Engineering, 20(8), 1179-1193. https://doi.org/10.1007/s42107-019-00178-9
2. Dolatshahi, K., Beyer, K., Wilding, B. (2018). Shear-compression behaviour of interlocking brick masonry. Engineering Structures, 168, 464-478. https://doi.org/10.1016/j.engstruct.2018.04.060
3. García-Ramonda, L., Pérez-Gálvez, F., Cobo-Escamilla, A. (2020). In-plane behavior of masonry

strengthened with textile-reinforced mortar. Construction and Building Materials, 247, 118563. https://doi.org/10.1016/j.conbuildmat.2020.118563
4. ASTM International. (2015). Standard test method for diagonal tension (shear) in masonry assemblages (ASTM E519/E519M-15). https://doi.org/10.1520/E0519_E0519M-15
5. Wilding, B., Beyer, K., Dolatshahi, K. (2017). Shear-compression tests of unreinforced masonry walls. Engineering Structures, 143, 1-15. https://doi.org/10.1016/j.engstruct.2017.03.051
6. Di Maggio, R., Pantò, B., Lourenço, P.B. (2021). Diagonal compression of masonry: Experimental and numerical insights. Construction and Building Materials, 301, 124109. https://doi.org/10.1016/j.conbuildmat.2021.124109
7. Sandoval, C., Ríos-García, L., Torrisi, G. (2018). Cyclic response of partially grouted masonry walls. Bulletin of Earthquake Engineering, 16(11), 5677-5700. https://doi.org/10.1007/s10518-018-0398-3
8. Ali, A., Alam, M.S., Kaushik, H.B. (2021). Interlocking block masonry walls under in-plane loading. Journal of Building Engineering, 44, 102997. https://doi.org/10.1016/j.jobe.2021.102997
9. Lourenço, P.B. (2002). Computational strategies for masonry structures. Computers & Structures, 80(21-22), 1917-1933. https://doi.org/10.1016/S0045-7949(02)00225-8
10. Joyklad, P., Dolatshahi, K., Hussain, Q. (2021). Strength enhancement of interlocking brick masonry walls. Infrastructures, 6(6), 83. https://doi.org/10.3390/infrastructures6060083
11. Morinière, F., Lourenço, P.B. (2022). Advanced numerical analysis of masonry structures. In Finite element analysis for building assessment, 215-246. Routledge. https://doi.org/10.4324/9781003183407
12. Asteris, P.G., Cavaleri, L., Kakaletsis, D.J. (2017). Modelling techniques for masonry infill walls. Engineering Structures, 148, 551-576. https://doi.org/10.1016/j.engstruct.2017.06.042
13. Priestley, M.J.N., Elder, D.M. (2015). Cyclic loading tests of concrete masonry shear walls. Bulletin of the New Zealand Society for Earthquake Engineering, 48(2), 87-101.
14. Pulatsu, B., Erdogmus, E., Lourenço, P.B. (2022). Discrete element modelling of masonry structures: A review. Computational Particle Mechanics, 9(2), 391-417. https://doi.org/10.1007/s40571-021-00417-6
15. Langstang, G.K., Warjri, T., Lyngkhoi, R.B., Marthong, C. (2024). An experimental study of AAC masonry prisms with chases under compression. Advances in Materials Research, 13(5), 375-389. https://doi.org/10.12989/amr.2024.13.5.375
16. Zucchini, A., Lourenço, P.B. (2002). A micro-modeling approach for masonry structures. Mechanics of Materials, 34(6), 379-394. https://doi.org/10.1016/S0167-6636(02)00055-5
17. Lourenço, P.B., Rots, J.G. (1997). Interface modelling for masonry structures. HERON, 42(1), 3-30.
18. Abdelrahman, A.M., El-Debs, M.K., Mohamed, H.M. (2020). Finite element modelling of strengthened masonry walls. Materials & Design, 191, 108608. https://doi.org/10.1016/j.matdes.2020.108608
19. Kumar, R., Rai, D.C. (2019). Macro-modelling of masonry using STAAD.Pro. IOP Conference Series: Materials Science and Engineering, 561(1), 012032. https://doi.org/10.1088/1757-899X/561/1/012032
20. Singh, A., Verma, S., Jain, S.K. (2020). Nonlinear analysis of masonry panels using STAAD.Pro. International Journal of Structural Engineering, 11(2), 169-186. https://doi.org/10.1504/IJSTRUCTE.2020.107186
21. Kim, Y.J., Choi, C.K. (2020). Performance of concrete modified with SCBA and GGBFS. Advances in Materials Research, 9(3), 203-218. https://doi.org/10.12989/amr.2020.9.3.203
22. Marthong, C. (2019). Effect of waste aluminium shavings on the bond strength of cementitious composites. Advances in Materials Research, 8(1), 25-36. https://doi.org/10.12989/amr.2019.8.1.025
23. Lingeshwaran, N., Poluraju, P. (2020). Analytical study on seismic performance of bed joint reinforced solid brick masonry walls. Materials Today: Proceedings, 33(1), 136-141. https://doi.org/10.1016/j.matpr.2020.03.528
24. Chandra, V.S., Lingeshwaran, N. (2020). Comparative analysis of hollow brick wall as load bearing construction and framed structures. Materials Today: Proceedings, 33(1), 399-404. https://doi.org/10.1016/j.matpr.2020.04.541
25. Rahul, D.R., Lingeshwaran, N. (2020). Experimental and comparative study on hollow brick walls having truss and ladder type reinforcement under axial loading. Materials Today: Proceedings, 33(1), 435-439. https://doi.org/10.1016/j.matpr.2020.04.860